CrossMark

# Preferential flow characteristics of reclaimed mine soils in a surface coal mine dump

**Lv Gang · Li Jun · Li Yexin · Wang Ting · Liu Yazhuo · Fu Xinyang**

**Abstract** There are a large number of macropores/tubular channels of a few centimeters and plant roots in reclaimed dump soils, which are the main reasons for the formation of soil macropores and soil preferential flow. To systematically study the morphological characteristics and variation of soil preferential flow for different reclaimed vegetations in a dump, a dye-staining experiment and physical and chemical analysis were carried out to investigate the formation mechanism and influencing factors of soil preferential flow in the vegetation restoration process. The results indicate that there were differences in the soil water breakthrough curves for different plots. The macropore effluent rate generally increased at first and then tended to stabilize. The soil steady effluent rate decreased with increasing soil depth, which reached the maximum and minimum values at the depths of 0~5 cm (0.0193~0.0315 mm s$^{-1}$) and 50~60 cm (0.0028~0.0035 mm s$^{-1}$), respectively. Furthermore, the radius of soil macropores under different types of reclaimed vegetation ranged from 0.03 to 4.71 mm, most of which ranged from 0.11 to 2.36 mm. The soil macroporosity of different reclaimed vegetation types ranged from 0.03 to 16.58%, which was significantly greater than 5%. The soil macroporosity determined 65% of the variation in the steady effluent rate and 42% of the

variation in the saturated hydraulic conductivity. Furthermore, the dye coverage ratio decreased as the soil layer depth increased in different plots, and there were some differences in each plot. The maximum dye coverage ratio occurred in the 0~5 cm soil layer, which reached 90.37%. The dye coverage ratio at a depth of 0~60 cm in six plots followed the order of *Robinia pseudoacacia* (26.48%) > *Ulmus pumila* (20.12%) > mixed forest (17.32%) > farmland (15.06%) > shrub (13.97%) > weeds (10.07%). The soil preferential flow mostly occurred in the 0~40 cm soil depth layer, which occupied more than 93% of the total soil profile (0~60 cm). Moreover, a Pearson correlation was used to analyze the relationship between environmental factors (soil, water, and plant factors) and the dye coverage ratio. The dye coverage ratio of soil preferential flow under different reclamation vegetations was very significantly or significantly positively correlated with the gravel content, mean radius of soil macropores, soil saturated hydraulic conductivity, root weight density, and root length density, which promoted the formation and development of soil preferential flow. This study will provide a scientific basis for understanding the formation mechanism and perfecting the research system of soil preferential flow, vegetation restoration, and reconstruction in a dump; furthermore, this research offers significance guidance in the construction of green mines and the development of regional economics.

L. Gang · L. Jun
College of Land and Environment, Shenyang Agricultural University, Shenyang, Liaoning 110866, China

L. Gang (✉) · L. Yexin · W. Ting · L. Yazhuo · F. Xinyang
College of Environmental Science and Engineering, Liaoning Technical University, Fuxin, Liaoning 123000, China
e-mail: lvgang2637@126.com

🠚 Springer

## Introduction

Preferential flow was defined as a phenomenon in which soil water moves along certain pathways, such as soil macropores, soil cracks, wormholes, and plant roots, bypassing most of the porous matrix and quickly moving through the soil media (Bauters et al. 2000; Hagedorn and Bundt 2002; Hendrickx and Flury 2001). Soil preferential flow was caused by the spatial heterogeneity of the soil structure, which existed in the process of soil water infiltration (Clothier et al. 2008; Miao et al. 2016a). The surroundings and imbalance were two important features of preferential flow (Zhang et al. 2016a). In structured soils, preferential flow existed along meso- and macropores (Beven and Germann 1982), whereas in non-structured soils, the channeling of rainfall on its way into the ground likely occurred as "fingered" flow (Glass et al. 1988). Preferential flow could promote the supplementation of soil water infiltration into groundwater, increase the risk of pesticides, fertilizers and other pollutants moving into the groundwater, reduce the utilization efficiency of rainfall and irrigation for plants, and weaken the ability of soil water conservation (Larsson et al. 1999; Miao et al. 2016b).

Soil macropores were considered the main determinant of preferential flow. Luxmoore (1981) found that soil macropores, including soil pores among soil aggregates, soil cracks caused by soil swelling-shrinkage, root channels, and soil animal channels, could provide a preferential path for soil water infiltration. Furthermore, soil macropores were distributed in aggregation. The formation of a preferential flow path was determined by the number and distribution characteristics of soil macropores in certain areas (Cheng et al. 2001; Luxmoore et al. 1990). The scope and number of soil macropore radius were calculated by water breakthrough curves in forest soil, and the corresponding characteristics were also analyzed (Radulovich 1989; Shi et al. 2005). Moreover, the morphological characteristics of soil macroporosity and preferential flow were observed with a dye staining experiment, and the distribution of a preferential path in the soil profile was established with image processing (Flury et al. 1994; Forrer et al. 2000; Gazis and Feng 2004; Wang and Zhang 2011). The formation of soil preferential flow was affected by both external and internal factors (Zhang et al. 2007). There are some factors affecting preferential flow, such as soil properties (Jørgensen et al.

2002; Koestel et al. 2012; Zavala et al. 2009), soil initial water content (Wang et al. 1999), gravel content (Herrick et al. 2010; Jomaa et al. 2012), rainfall intensity (Dušek et al. 2006; Yan and Zhao 2016; Miao et al. 2015), and plant roots (Hangen et al. 2005; Stewart et al. 1999; Zhang et al. 2015). The soil water content could influence the soil water infiltration ability by changing the potential soil gradients, thus influencing the distribution of preferential flow. Preferential flow was also affected by the content, size, position, lithology, and other characteristics of gravel. Plant roots can form a series of root channels in the soil that promote the formation of preferential flow.

The formation and development of preferential flow can influence surface runoff, deep soil water distribution, and groundwater level. Water and soil nutrients will enter the deep soil and groundwater with preferential flow, which result in the redistribution and inhomogeneity of water pressure in the soil, thus causing geologic hazards, such as collapse, landslides, and debris flow. However, most of the studies in China have focused on preferential flow on forest lands and farmland (Yan and Zhao 2016) and the influence of soil cracks on preferential flow (Zhang et al. 2016b), while few studies have focused on the distribution and characteristics of preferential flow in reclaimed dump soils with different vegetations. During the mining process at the surface coal mine, the land was excavated and occupied, the vegetation was destroyed, animal and plant habitats were influenced, and the natural hydrological, geological, and geomorphological conditions were also destroyed. The dump was a typical loose engineering spoil, and it has compaction platform, loose slope, complex material composition, and special soil macrospores. Thus, the dump was the most serious soil erosion area of surface coal mines. Furthermore, the dump was mostly located in eco-environmentally fragile areas with poor climate, water, nutrient conditions, and vegetation coverage. Moreover, the dump had typical reconstructed soil with loose structure, lower capacity for water storage, and developed soil macropores, which resulted in the loss of soil water and nutrients.

In this study, six areas of the Haizhou surface coal mine dump in Fuxin, China, were reclaimed with similar reconstruction techniques; however, differing vegetation types were studied to compare the characteristics of soil macropore radius and preferential flow. The objectives of this study were as follows: (i) to define the scope and number of soil macropore radius; (ii) to

study the distribution of preferential flow within the soil profile; and (iii) to investigate the main influencing factors of preferential flow for the different reclaimed vegetation types.

## Materials and methods

### Study site

The study was conducted at the Haizhou surface coal mine dump, which has an area of 16 km$^2$ and is located in Fuxin city, Liaoning Province, China (Fig. 1). The climate was semi-arid and semi-humid, with an average annual rainfall of 550 mm, 79% of which occurs between June and September. The average annual evaporation was 1700 mm. The average annual temperature was 9.5 °C. In 2004, the area was reclaimed by being covered with natural soil to a depth of 30 cm. This study was carried out in April of 2012.

Considering factors such as the vegetation type, topographic features, and discarding process, six reclaimed vegetation types, which were located in the same region of the dump and without influence among them, were selected as study objects. The reclamation types included *Robinia pseudoacacia* (A), *Ulmus pumila* (B), mixed forest (*R. pseudoacacia* and *U. pumila*,C), shrub (*Amorpha fruticosa* Linn, D), farmland (crop, E), and weeds (F). The vegetation restoration characteristics of each plot were studied by setting the standard ground. The standard ground of *R. pseudoacacia*, *U. pumila*, and mixed forest was 20 m × 20 m. The standard ground of the shrub and weeds was 10 m × 10 m and 5 m × 5 m, respectively (Table 1).

### Experimental measurements

#### Determination of soil macropores

Soil samples were collected by using steel cutting rings (5 cm in height; 200 cm$^3$ in volume) in the field for an indoor seepage experiment to obtain a water breakthrough curve. The equivalent radius, number, and distribution of the large pores were calculated according to the *Poiseuille* equation.

(1)  Basic principal
     For this study, macropores were defined as

pores that drained when the soil reached field capacity, and our work concentrated on pores draining as the soil passed from saturation to field capacity. When the soil moisture content reached field capacity, the soil water infiltration capacity mainly depended on the water supply intensity. Typically, the soil pores were hypothesized to be circular, with an aperture of $r$. Thus, the flow rate could be calculated by using the *Poiseuille* equation

$$Q = \pi r^4 \Delta p \big/ (8 \eta \tau L) \tag{1}$$

For the steady flow, the formula could be simplified as follows

$$Q = \pi \tau r^2 L \big/ t \tag{2}$$

where $Q$ was the unit discharge (cm$^3$ s$^{-1}$); $\tau$ was the ratio of the actual path and the length of the soil column, 1.2 in this study; $\eta$ was the mean viscosity coefficient of water (g cm$^{-1}$ s$^{-1}$); $r$ was the mean pore radius (cm); $\Delta p$ was the mean pressure head (cm); $t$ was the start time of water first being adding (s); and $L$ was the mean soil column length (cm).

When the soil moisture content reached field capacity, the water in the macropore first drained out, leading to a gradual change to a relatively smaller radius of the macropore. The radius after the first drainage was set as the maximum. The radius of the initial drainage in the soil pore was set as the maximum pore radius, and the radius of the steady flow in the soil pore was set as the minimum pore radius. The equivalent radius of the macropores could be calculated according to the following formula

$$r = \tau L \Big[ 8 \eta \big/ (t \Delta p) \Big]^{1/2} \tag{3}$$

The radius of the soil pore during arbitrary periods was calculated according to formula (3). The relationship of soil macropore discharge $Q$ with radius area $S$ and flow velocity $v$ was as follows

$$Q = nSv = n \pi r^2 v \tag{4}$$

Thus, when the flow $Q$ was known, the number of macropores $n$ can be calculated following formula (4).
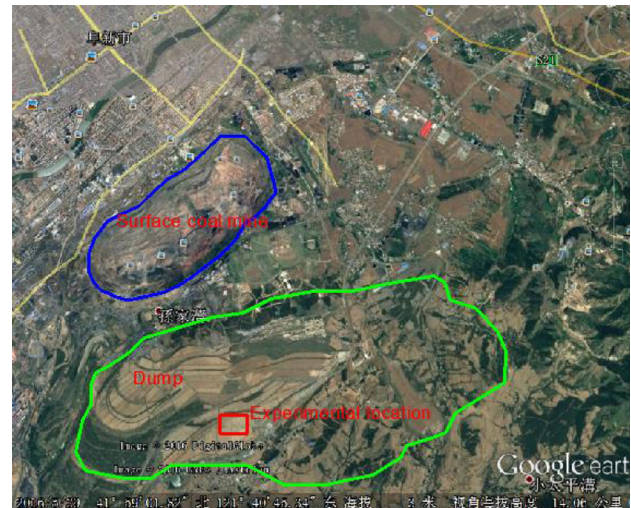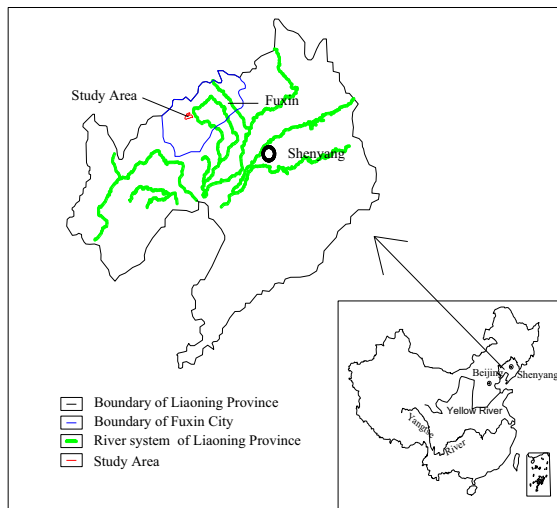
**Fig. 1** Location of the study area

According to the above equations, the following values could be obtained:

1) The maximum pore radius of the soil samples was calculated according to Eq. (3), where $\tau$ was 1.l; the minimum pore radius was calculated according to Eq. (2), where $\tau$ was 1.2. The $\tau$ value in arbitrary periods could be obtained with an interpolation method, and then, the relative macropore radius could be calculated according to formula (3).

2) The number of the average radius $r$ could be calculated by the measured discharge and formula (4).

3) The macropore area could be calculated according to the average radius of $r$.

4) The macropore volume in an arbitrary range was the product of the size of the area and the length of the soil column, and the macropore proportion could be calculated.

(2) Methods

The soil macropores were measured by using a Markov bottle, where the water head height was kept at 1 cm. Timing began when the first drops were drained, which were measured at 5 s intervals. All of the experimental treatments had the same run time of 120 s.

**Table 1** The basic profiles in all plots

| Index | | Robinia pseudoacacia (A) | Ulmus pumila (B) | Mixed forests (C) | Shrub (D) | Farmland (E) | Weeds (F) |
|---|---|---|---|---|---|---|---|
| Geographical position | N | 41° 57′ 22.39″ | 41° 57′ 27.42″ | 41° 57′ 36.62″ | 41° 57′ 11.75″ | 41° 57′ 43.34″ | 41° 57′ 06.89″ |
| | E | 121° 39′ 40.09″ | 121° 40′ 08.64″ | 121° 40′ 06.76″ | 121° 39′ 26.62″ | 121° 40′ 06.37″ | 121° 39′ 51.26″ |
| Altitude (m) | | 263.30 | 268.50 | 234.7 | 262.0 | 262.5 | 258.8 |
| Small terrain | | Flatland | Flatland | Flatland | Flatland | Flatland | Flatland |
| Water source | | Precipitation | Precipitation | Precipitation | Precipitation | Precipitation | Precipitation |
| Litter thickness (cm) | | 1~2 | 2~3 | 1~2 | 0.5~1 | 0 | 0.5~1 |
| Cover of litter (%) | | 98 | 99 | 60 | 60 | 0 | 95 |
| coverage of tree stories (%) | | 65 | 65 | 70 | 65 | 0 | 0 |
| Total plant cover (%) | | 99 | 96 | 99 | 98 | 5 | 97 |
| Soil and water loss | | Moderate | Moderate | Moderate | Moderate | Moderate | Moderate |

*Dye staining experiment*

(1)  Experimental preparation

A study plot (65 cm × 65 cm) was chosen in each reclaimed-vegetation type, and the rocks and litter were removed with a small shovel. Then, four pieces of metal with a size of 65 cm × 50 cm were buried in the soil and kept in a box shape, which was elevated 20 cm above the soil surface and 30 cm under the soil surface. To improve the test accuracy, the soil within 5 cm of the inside frame could be compacted (Fig. 2). All of the experiments were replicated three times.

(2)  Dyeing tracer

Brilliant Blue FCF (BB) dye was used in this study due to its good visibility in soils, low toxicity, low sorption, and transport properties similar to water (Germán-Heins and Flury 2000). In each plot, a total of 32 L of dye solution, with a concentration of 4 g $L^{-1}$, was poured into the closed box shape with ponding infiltration.

(3)  Profile excavation and soil sample collection

The canvas was removed 24 h into the dye staining experiment, and the soil profile was excavated in the middle of the 50 cm × 50 cm region. Then, a vertical acquisition dyeing profile was obtained using a digital camera with 12 million pixels after dressing the soil profile, and 3~5 photos were selected for the next picture process.

The soil samples were measured at 10 cm intervals at a depth of 0~60 cm, whereas the 0~10 cm soil layer was divided into 0~5 and 5~10 cm, respectively. The soil water content, soil bulk density, porosity (total porosity, capillary porosity, and non-capillary porosity), and saturated hydraulic conductivity were measured using the ring method. The gravel content was mass percent, and it was measured by washing methods. Then, 1 kg of soil sample was collected in each soil layer and taken to the laboratory for further analysis (Institute of Soil Science 1978). All experiments were replicated three times.

The roots were collected at 10 cm intervals by using a root drilling method (10 cm diameter and 10 cm length), which was located at a distance of 30 cm away from the standard plant in each plot. The root samples were cleaned from root drilling in the laboratory. Then, the roots were classified by root diameter <1, 1~2, and 2~5 mm. The root length was determined using the WinRHIZO PRO 2009 software (Regent Inc., Canada). The root biomass was weighted after being oven-dried at 75 °C (Table 2).

(4)  Dyeing image processing

The dye coverage was determined based on the soil profile images according to the following description. These images were processed with Photoshop 11.0, and several steps were necessary in order to obtain diagrams that could express the depth and proportion of the stained area. (1) The soil profile images were input into Photoshop 11.0, and the images that could not be photographed orthogonally were deskewed based on the steel rulers in the pictures. Then, the stained areas along the boundaries between stained areas and unstained areas were vectorized, and the stained areas were filled with white color. (2) A scale for the stained profiles was added, which were transformed to TIF format images. (3) The total pixels (P) of an image from the histogram were checked; then, all of the white areas were selected with the magic wand to obtain the pixels (P1) of the stained areas. The dye coverage ratio, the ratio of P1 to P in the image, was used to quantitatively describe the preferential flow morphological characteristics.

## Results

### Soil water breakthrough curve characteristics

The macropore effluent rate generally increased at first and then tended to be stable in 60~80 s, finally reaching a stable state in 100 s (Fig. 4). There were differences in the soil water breakthrough curves in different plots. The soil effluent rate was relatively high at a depth of 0~5 cm in the arbor forest. The steady effluent rate under *R. pseudoacacia*, *U. pumila*, and mixed forest was 0.0281, 0.0292, and 0.0315 mm $s^{-1}$, respectively, whereas the steady effluent rate under shrubs, farmland, and weeds was lower than 0.02 mm $s^{-1}$, and the steady effluent rate under waste grasslands was the lowest (0.0193 mm $s^{-1}$). The steady effluent rate was closely related to reclamation vegetation growth and the improved effect of its root on soil structure at the dump.

**Fig. 2** Diagram of experimental installation for the Brilliant Blue FCF dye staining experiment
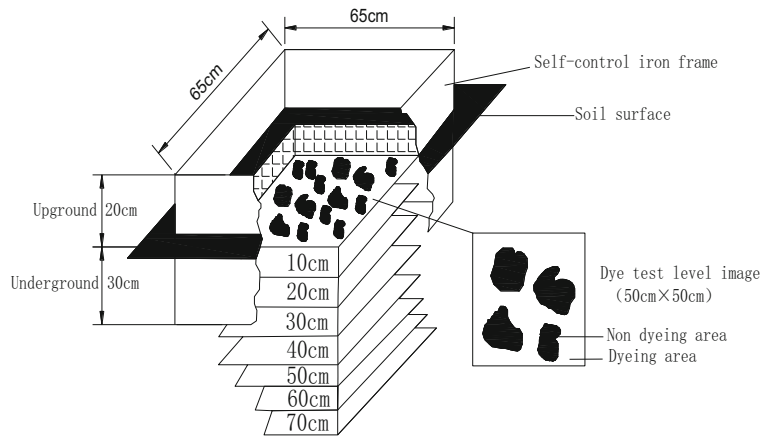


For all six plots, the steady soil effluent rate decreased with an increase in the soil depth, which reached the minimum and maximum values at the depths of 0~5

and 50~60 cm, respectively. For *R. pseudoacacia* (A), there were differences in the soil water breakthrough curve in different soil layers and changes to the time

**Fig. 3** The dyeing test process and image processing



Brilliant Blue FCF Configurated

Brilliant Blue FCF added

Sample layout

Brilliant Blue FCF infiltration

Acquisition vertical dyeing profile

Image processing
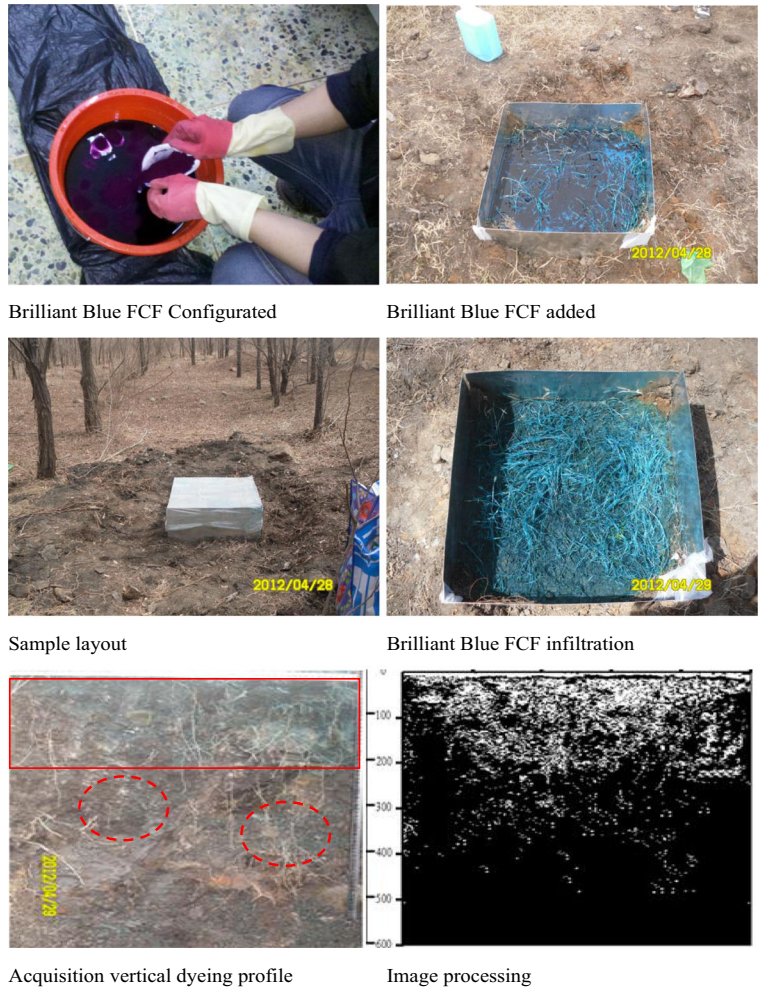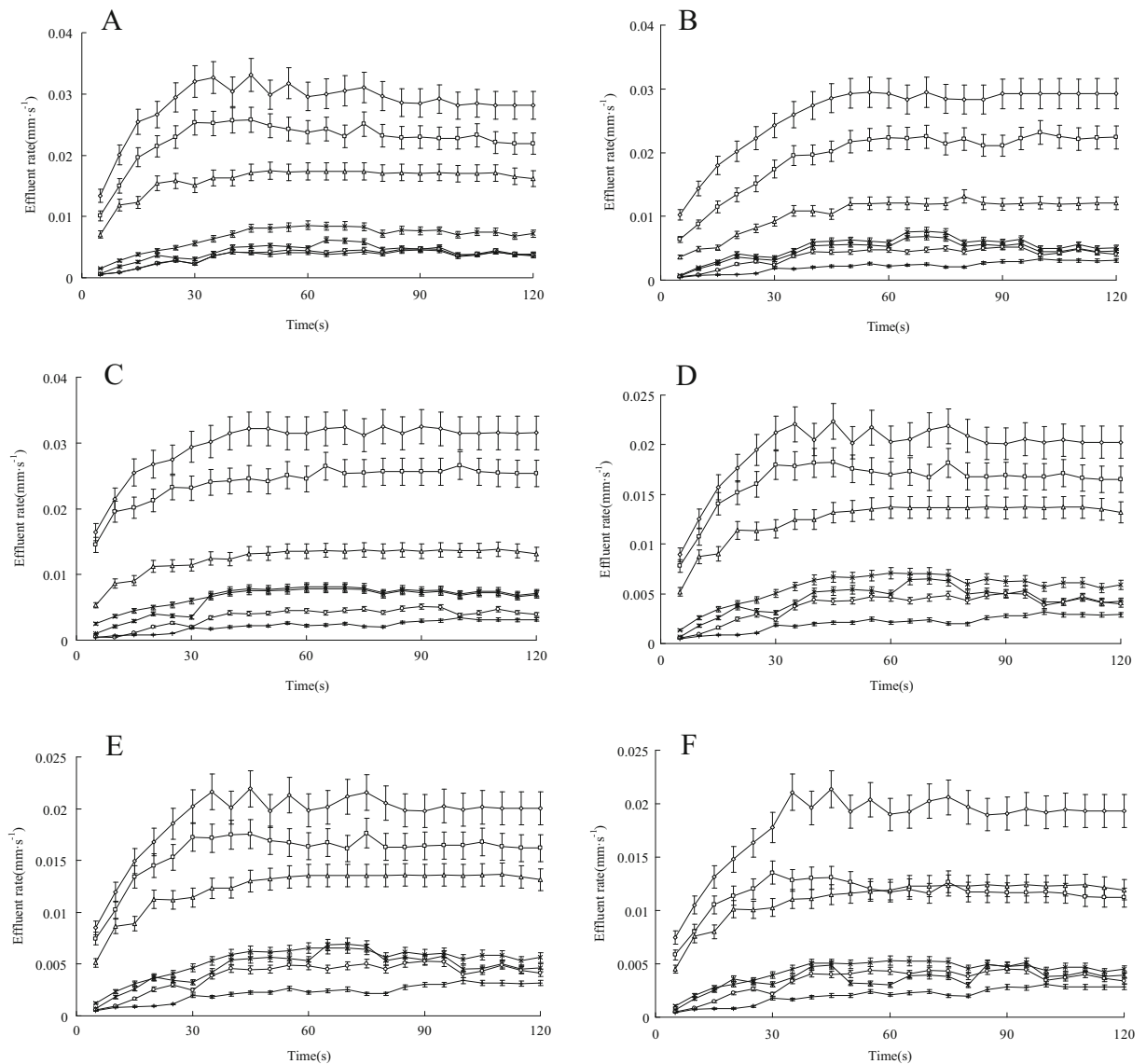
**Fig. 4** Soil water breakthrough curve in the different plots

required to reach a steady effluent rate. The soil at a depth of 0~10 cm reached a stable flow in the 80 s, whereas the soil at a depth of 10~60 cm reached a stable flow in 60 s. The soil water breakthrough curve in the different soil layers had different fluctuation degrees. The soil water fluctuated less at 10~60 cm, whereas it fluctuated relatively dramatically at 0~10 cm, especially at 0~5 cm. According to the changing processes of the soil water characteristic curve, the effluent rate can be divided into an active phase, a fluctuation phase, and a stable phase. The active phase occurred at 0~30 s; the effluent rate rapidly increased from the initial

0.0134 mm s$^{-1}$ (5 s) to 0.0320 mm s$^{-1}$ (30 s), with a growth rate of 139.28%. The fluctuation period occurred between 30 and 90 s, and the effluent rate fluctuated to different degrees, ranging from 0.0285 to 0.0331 mm s$^{-1}$. The stable phase occurred between 90 and 120 s, when the effluent rate was 0.0281 mm s$^{-1}$. The steady effluent rate was different in the different soil layers and followed the order of 0~5 cm (0.0281 mm s$^{-1}$) > 5~10 cm (0.0219 mm s$^{-1}$) > 10~20 cm (0.0162 mm s$^{-1}$) > 20~30 cm (0.0072 mm s$^{-1}$) > 30~40 cm
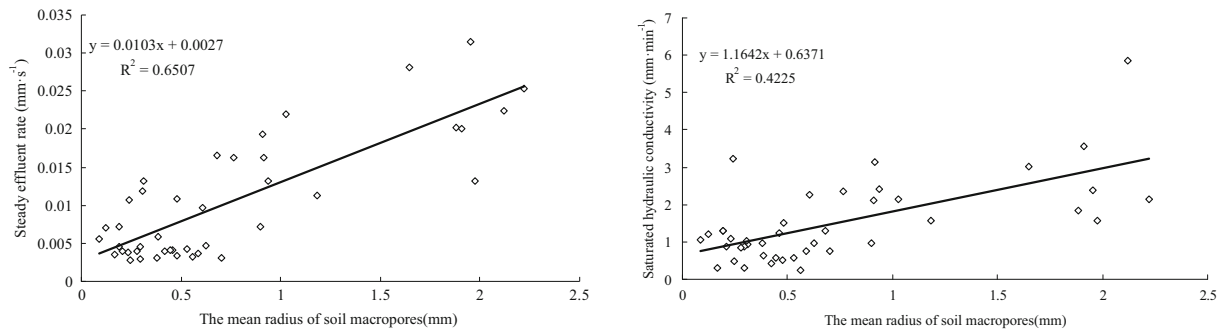
**Fig. 5** The relationship between the mean radius of soil macropores with the steady effluent rate and saturated hydraulic conductivity
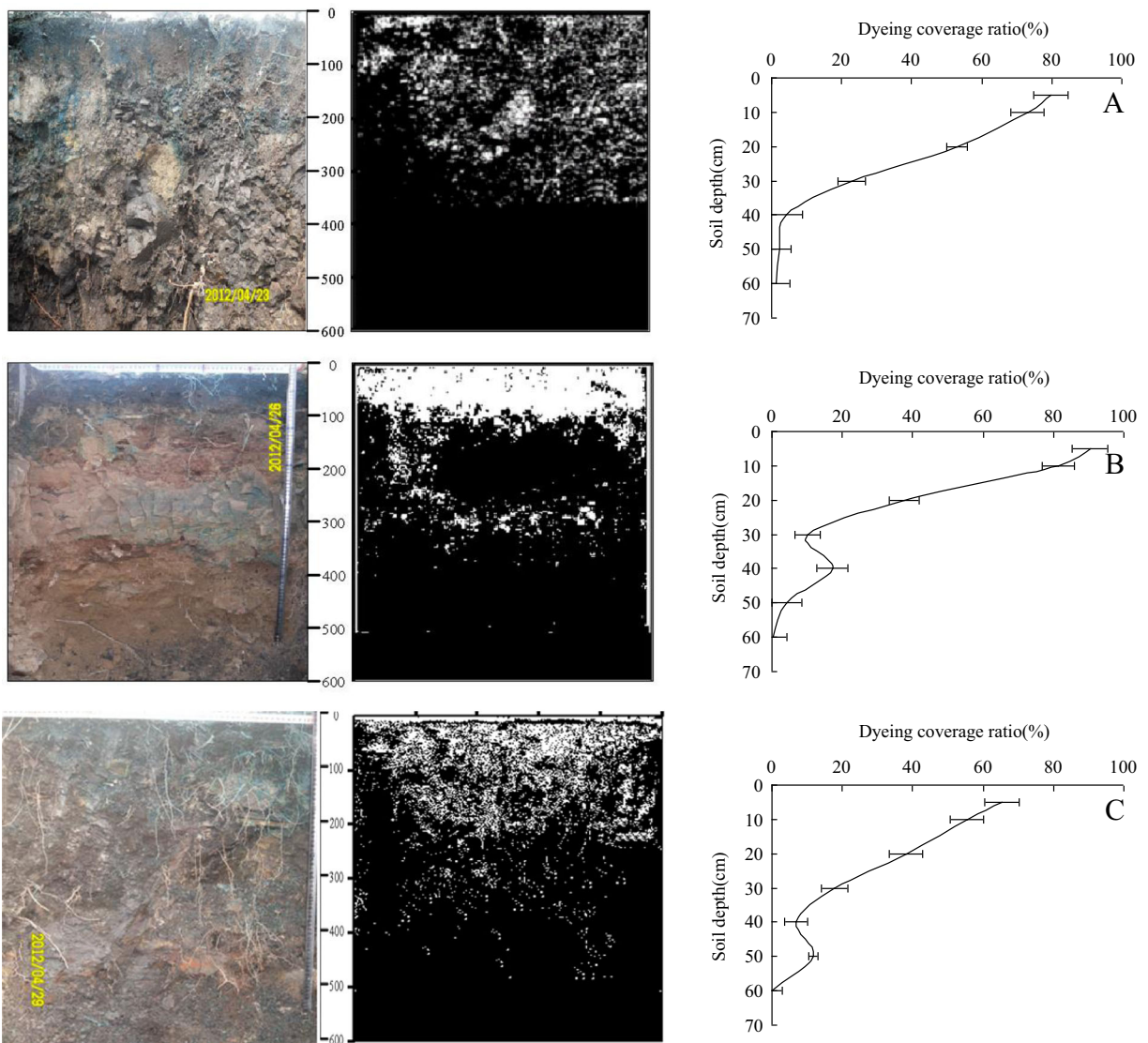


**Fig. 6** Image of soil preferential flow characteristics in different plots
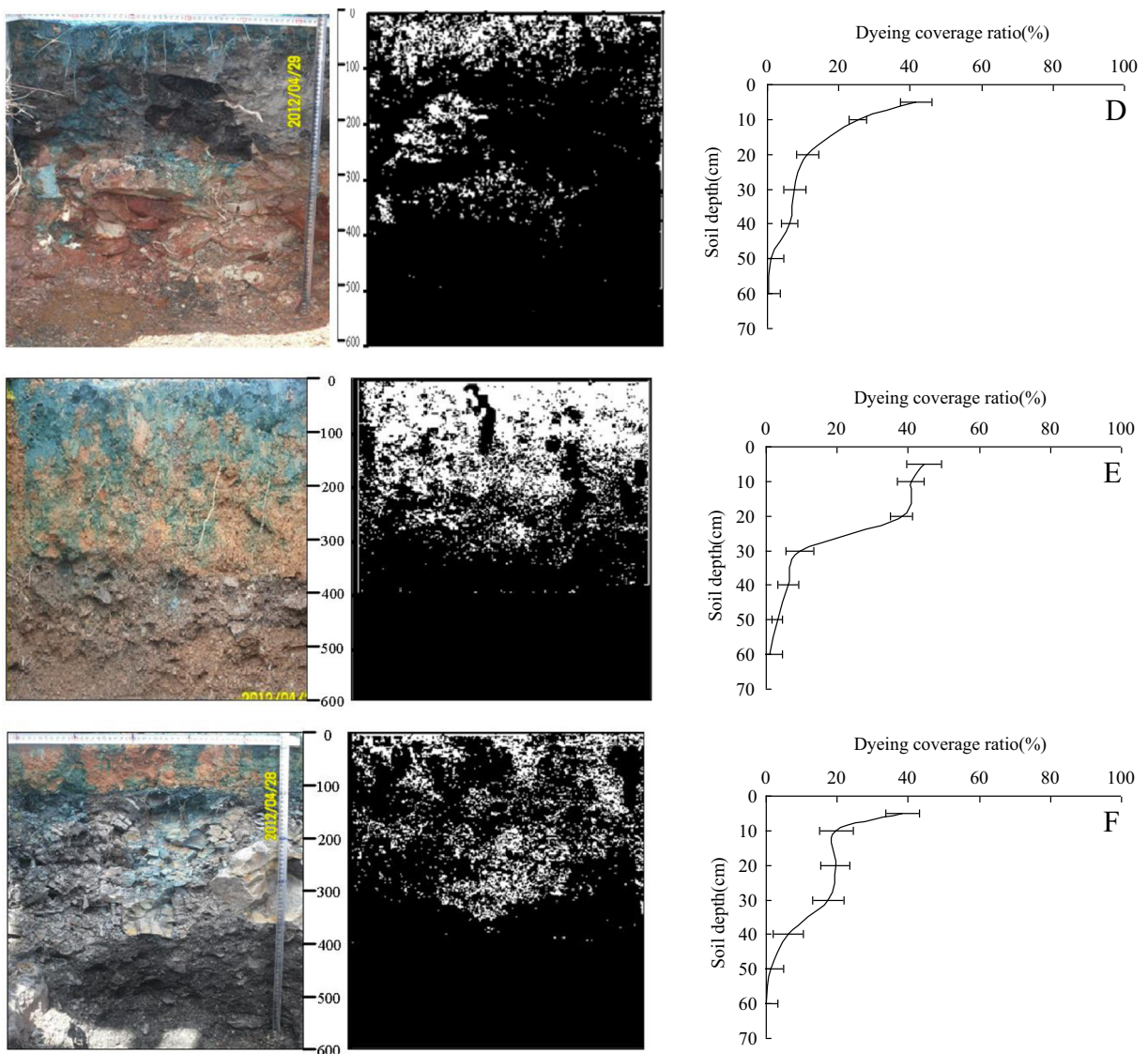
**Fig. 6** (continued)

$(0.0039 \text{ mm s}^{-1}) > 40\sim50 \text{ cm}$ $(0.0037 \text{ mm s}^{-1}) > 50\sim60 \text{ cm} (0.0035 \text{ mm s}^{-1})$. The steady effluent rate at $0\sim5$ cm was significantly greater than that in the other soil layers, and it was eight times that at $50\sim60$ cm.

The scope and density of soil macropores

The scope of the minimum radius was different from that of the maximum radius between the field capacity and saturated water content (Table 3). The minimum radius of the six samples were $0.10\sim0.15$ mm, $0.03\sim0.04$ mm, $0.03\sim0.04$ mm, $0.18\sim0.20$ mm, $0.03\sim0.04$ mm, and $0.19\sim0.22$ mm; the maximum radius of the six samples were $1.00\sim3.23$ mm, $0.61\sim1.92$ mm, $2.11\sim4.71$ mm, $0.79\sim1.36$ mm, $2.11\sim4.71$ mm, and $2.11\sim4.71$ mm. There were no significant differences in the radius and the number of soil macropores in the different soil layers for all six plots. The scope of the soil macropore radius of the lower soil was greater than that in the upper layer. For *U. pumila* (B), the macropore radius in each of the soil layers of $0\sim60$ cm was $0.12\sim0.43$ mm, $0.10\sim0.43$ mm, $0.11\sim0.43$ mm, $0.14\sim0.43$ mm, $0.16\sim0.96$ mm, $0.40\sim3.23$ mm, and $0.12\sim0.43$ mm, with an average size of 0.17, 0.16, 0.20, 0.19, 0.23, 0.59, and 0.17 mm,
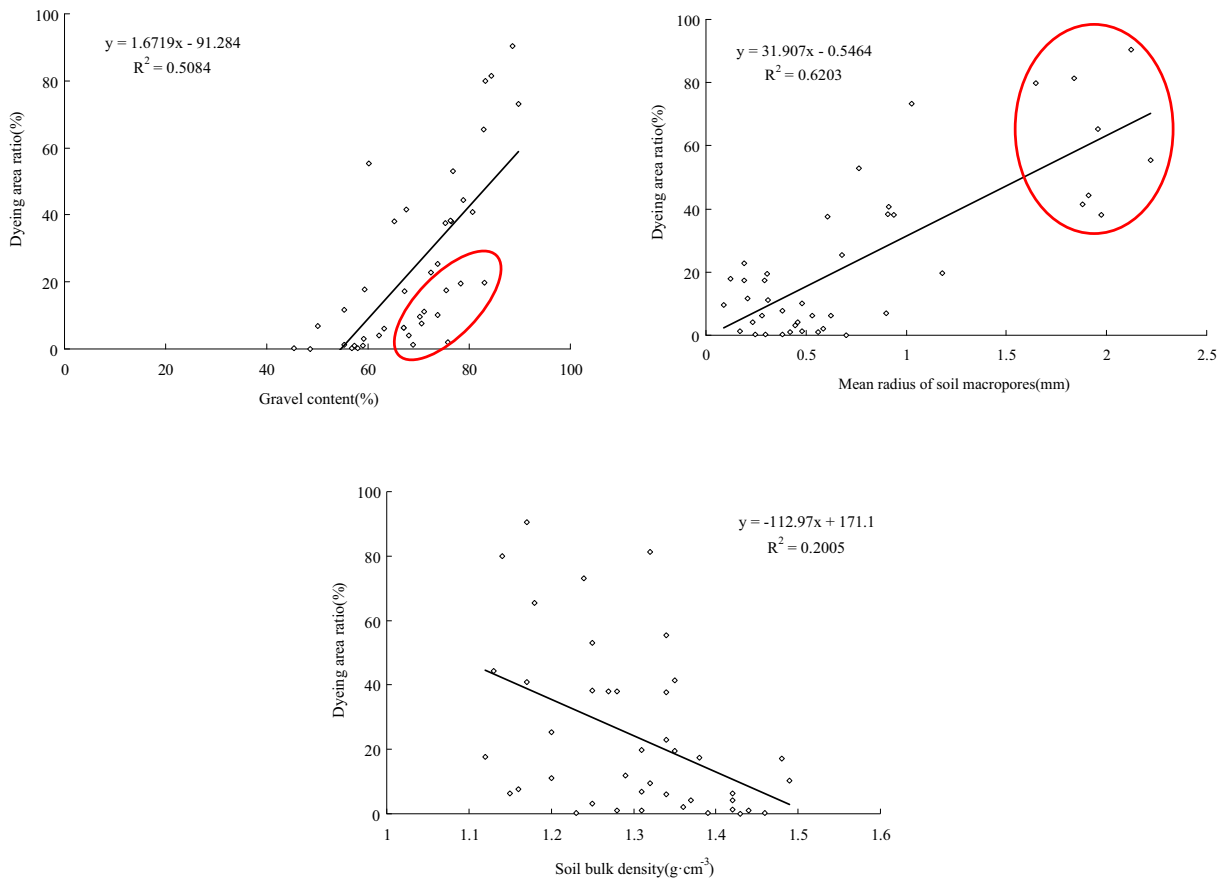
**Fig. 7** The relationship between the dye coverage ratio and soil factors

respectively. There was no significant difference in the average radius of the soil macropores in the 0~40 mm soil layer ($P < 0.05$), which suddenly increased in the 40~50 cm soil layer and then decreased to 0.17 mm in the 50~60 cm soil layer.

Effects of soil macropores on the effluent rate and saturated hydraulic conductivity

There was a very significant positive correlation between the average radius of the soil macropores with a
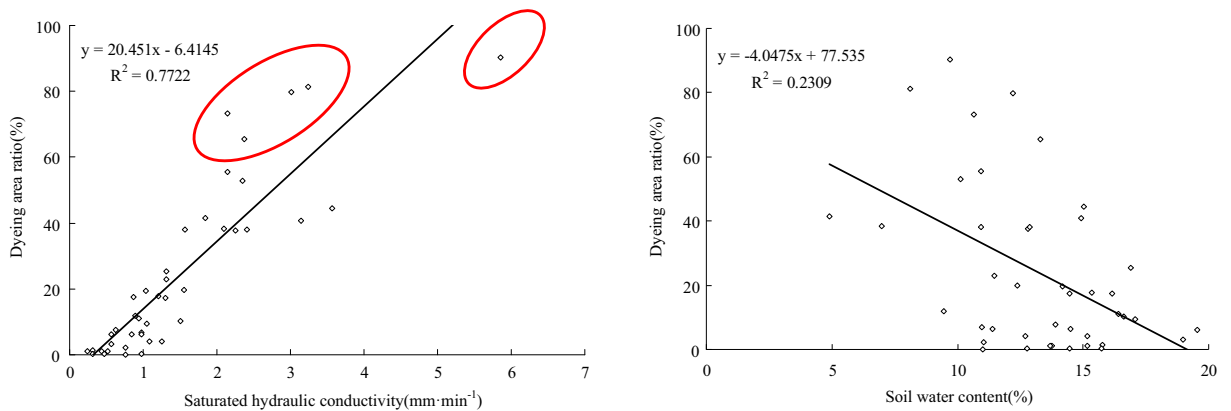


**Fig. 8** The relationship between the dye coverage ratio and water factors
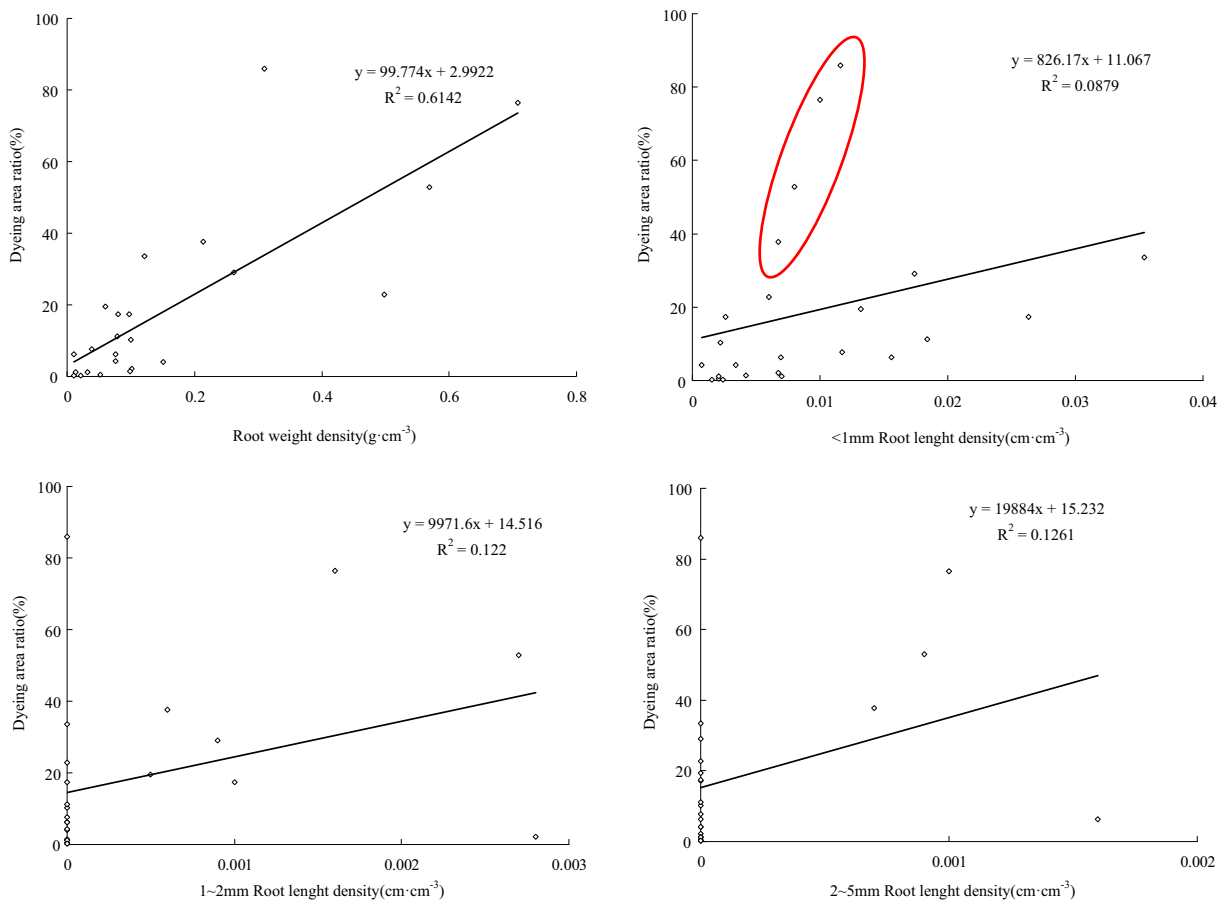
**Fig. 9** The relationship between the dye coverage ratio and plant factors

steady effluent rate and saturated hydraulic conductivity ($P < 0.01$; Fig. 5). The soil macroporosity with different reclaimed vegetations at the dump ranged from 0.03 to 16.58%, which was greater than 5%. The soil macropores determined 65% of the variation in the steady effluent rate and 42% of the variation in the saturated hydraulic conductivity.

The occurrence and morphological characteristics of soil preferential flow

There were differences in the preferential flow characteristics among the different plots (Fig. 6). The preferential flow in each plot mostly occurred in the 0~40 cm soil layer, which occupied 98.54% (A), 98.12% (B), 93.93% (C), 98.53% (D), 97.09% (E), and 98.71% (F) of the whole soil profile. The dye coverage ratio under the arbor decreased as the soil layer increased. The dye coverage ratio under *R. pseudoacacia* was less than 5% when the soil layer depth was below 40 cm. However,

the dye coverage ratio under the *U. pumila* and mixed forest slightly increased at depths of 40~50 cm and 50~60 cm, respectively; the ratios were 17.28 and 11.76%, respectively. There was no obvious variation in the dye coverage ratio at a depth of 0~20 cm on farmland, which ranged from 38.11 to 44.36%. Compared with the dye coverage ratio at a depth of 10~20 cm, the dye coverage ratio at 20~30 cm decreased by 75.02% and reached 9.52%. This indicated that when the preferential flow came close to or reached the bottom of the soil, it was affected by the soil layer.

For *R. pseudoacacia*, the preferential flow mainly occurred at a depth of 0~35 cm, the front part (the maximum migration depth) could reach approximately 38 cm, and the dye coverage ratio was 26.48%. The dye coverage ratio of each layer was 79.84% (0~5 cm), 73.19% (5~10 cm), 52.92% (10~20 cm), 22.86% (20~30 cm), 4.12% (30~40 cm), 2.15% (40~50 cm), and 1.31% (50~60 cm). From the profile images of *R. pseudoacacia*, the preferential flow pathways were

**Table 2**  The basic physical properties in each plot in the study area

| Plots | Depth (cm) | PD (%) Sand (%) | Silt (%) | Clay (%) | GC (%) | BD (g cm$^{-3}$) | CP (%) | SHC (mm min$^{-1}$) | RWD (g cm$^{-3}$) | RLD (cm cm$^{-3}$) <1 mm | 1–2 mm | 2–5 mm |
|---|---|---|---|---|---|---|---|---|---|---|---|---|
| A | 0–5 | 6.06 | 10.35 | 0.35 | 83.24 | 1.14 | 40.64 | 3.01 | 0.7076 | 0.0100 | 0.0016 | 0.0010 |
|   | 5–10 | 7.28 | 2.51 | 0.40 | 89.81 | 1.24 | 39.64 | 2.14 |  |  |  |  |
|   | 10–20 | 17.83 | 4.66 | 0.65 | 76.86 | 1.25 | 38.09 | 2.35 | 0.5685 | 0.0080 | 0.0027 | 0.0009 |
|   | 20–30 | 25.32 | 1.85 | 0.36 | 72.47 | 1.34 | 39.57 | 1.31 | 0.4983 | 0.0060 | 0 | 0 |
|   | 30–40 | 22.27 | 7.66 | 1.96 | 68.11 | 1.37 | 44.87 | 1.08 | 0.1507 | 0.0007 | 0 | 0 |
|   | 40–50 | 19.86 | 3.72 | 0.61 | 75.81 | 1.36 | 37.07 | 0.76 | 0.1021 | 0.0067 | 0.0028 | 0 |
|   | 50–60 | 25.82 | 4.45 | 0.89 | 68.84 | 1.42 | 41.13 | 0.31 | 0.0985 | 0.0042 | 0 | 0 |
| B | 0–5 | 6.42 | 4.34 | 0.68 | 88.56 | 1.17 | 45.03 | 5.86 | 0.3100 | 0.0116 | 0 | 0 |
|   | 5–10 | 10.64 | 4.17 | 0.86 | 84.33 | 1.32 | 31.13 | 3.24 |  |  |  |  |
|   | 10–20 | 22.00 | 2.42 | 0.36 | 75.22 | 1.34 | 33.51 | 2.25 | 0.2131 | 0.0067 | 0.0006 | 0.0007 |
|   | 20–30 | 22.23 | 3.43 | 0.54 | 73.80 | 1.49 | 35.12 | 1.51 | 0.1003 | 0.0022 | 0 | 0 |
|   | 30–40 | 25.54 | 6.31 | 0.86 | 67.29 | 1.48 | 32.51 | 1.30 | 0.0977 | 0.0263 | 0.0010 | 0 |
|   | 40–50 | 33.31 | 4.04 | 0.49 | 62.16 | 1.42 | 34.68 | 1.25 | 0.0758 | 0.0034 | 0 | 0 |
|   | 50–60 | 34.70 | 7.35 | 1.13 | 56.82 | 1.39 | 37.88 | 0.98 | 0.0521 | 0.0021 | 0 | 0 |
| C | 0–5 | 6.32 | 10.52 | 0.31 | 82.85 | 1.18 | 45.70 | 2.37 | nd | nd | nd | nd |
|   | 5–10 | 32.10 | 6.62 | 1.12 | 60.16 | 1.34 | 37.42 | 2.15 | nd | nd | nd | nd |
|   | 10–20 | 28.77 | 5.04 | 0.96 | 65.23 | 1.28 | 37.73 | 1.57 | nd | nd | nd | nd |
|   | 20–30 | 30.13 | 9.35 | 1.11 | 59.41 | 1.12 | 46.79 | 1.21 | nd | nd | nd | nd |
|   | 30–40 | 40.96 | 8.02 | 0.86 | 50.16 | 1.31 | 35.60 | 0.98 | nd | nd | nd | nd |
|   | 40–50 | 35.85 | 7.79 | 1.00 | 55.36 | 1.29 | 40.36 | 0.89 | nd | nd | nd | nd |
|   | 50–60 | 42.88 | 7.27 | 1.34 | 48.51 | 1.43 | 42.17 | 0.76 | nd | nd | nd | nd |
| D | 0–5 | 24.72 | 6.97 | 0.74 | 67.57 | 1.35 | 40.52 | 1.84 | 0.1218 | 0.0354 | 0 | 0 |
|   | 5–10 | 21.63 | 4.01 | 0.63 | 73.73 | 1.20 | 39.75 | 1.31 |  |  |  |  |
|   | 10–20 | 21.01 | 6.04 | 1.80 | 71.15 | 1.20 | 50.92 | 0.94 | 0.0786 | 0.0184 | 0 | 0 |
|   | 20–30 | 25.75 | 2.93 | 0.67 | 70.65 | 1.16 | 48.07 | 0.63 | 0.0393 | 0.0117 | 0 | 0 |
|   | 30–40 | 25.70 | 5.24 | 1.92 | 67.14 | 1.15 | 50.30 | 0.57 | 0.0756 | 0.0156 | 0 | 0.0016 |
|   | 40–50 | 36.93 | 3.44 | 0.62 | 59.01 | 1.28 | 46.93 | 0.43 | 0.0325 | 0.0070 | 0 | 0 |
|   | 50–60 | 36.10 | 5.52 | 0.47 | 57.91 | 1.23 | 45.76 | 0.31 | 0.0215 | 0.0024 | 0 | 0 |
| E | 0–5 | 14.25 | 6.30 | 0.70 | 78.75 | 1.15 | 39.06 | 3.57 | nd | nd | nd | nd |
|   | 5–10 | 11.50 | 6.88 | 0.99 | 80.63 | 1.17 | 42.64 | 3.15 | nd | nd | nd | nd |
|   | 10–20 | 17.88 | 4.87 | 0.70 | 76.55 | 1.15 | 44.84 | 2.41 | nd | nd | nd | nd |
|   | 20–30 | 24.51 | 4.18 | 1.06 | 70.25 | 1.32 | 41.68 | 1.05 | nd | nd | nd | nd |
|   | 30–40 | 28.98 | 7.28 | 0.58 | 63.16 | 1.34 | 31.10 | 0.98 | nd | nd | nd | nd |
|   | 40–50 | 35.01 | 5.28 | 0.48 | 59.23 | 1.25 | 35.63 | 0.57 | nd | nd | nd | nd |
|   | 50–60 | 30.74 | 10.29 | 1.65 | 57.32 | 1.31 | 24.41 | 0.24 | nd | nd | nd | nd |
| F | 0–5 | 13.08 | 9.38 | 1.24 | 76.30 | 1.25 | 35.88 | 2.10 | 0.2617 | 0.0174 | 0.0009 | 0 |
|   | 5–10 | 11.53 | 4.79 | 0.68 | 83.00 | 1.31 | 38.85 | 1.56 |  |  |  |  |
|   | 10–20 | 17.15 | 3.95 | 0.62 | 78.28 | 1.35 | 38.24 | 1.04 | 0.0603 | 0.0132 | 0.0005 | 0 |
|   | 20–30 | 21.15 | 3.04 | 0.42 | 75.39 | 1.38 | 34.83 | 0.87 | 0.0804 | 0.0026 | 0 | 0 |
|   | 30–40 | 27.44 | 4.67 | 0.85 | 67.04 | 1.42 | 36.57 | 0.84 | 0.0110 | 0.0069 | 0 | 0 |
|   | 40–50 | 40.92 | 3.47 | 0.29 | 55.32 | 1.44 | 44.54 | 0.52 | 0.0137 | 0.0021 | 0 | 0 |
|   | 50–60 | 45.98 | 7.89 | 0.79 | 45.34 | 1.46 | 40.02 | 0.47 | 0.0102 | 0.0015 | 0 | 0 |

*PD* particle-size distribution (sand (0.02–2 mm), silt (0.002–0.02 mm), clay (0–0.002 mm)), *GC* gravel content (>2 mm), *BD* bulk density, *CP* capillary porosity, *SHC* saturated hydraulic conductivity, *RWD* root weight density, *RLD* root length density, *nd* no data

**Table 3** The scope and number of soil macropores radius

| Plots | Depth (cm) | Radius ranges (mm) | Number ($10^6$) | Radius ranges (mm) | Number ($10^6$) | Radius ranges (mm) | Number ($10^6$) |
|---|---|---|---|---|---|---|---|
| A | 0~5 | 0.12–0.15 | 86.09 | 0.16–0.19 | 30.99 | 0.22–0.43 | 17.22 |
| | 5~10 | 0.10–0.15 | 215.23 | 0.16–0.19 | 60.32 | 0.22–0.43 | 37.22 |
| | 10~20 | 0.11–0.14. | 55.39 | 0.16–0.19 | 44.39 | 0.22–0.43 | 38.22 |
| | 20~30 | 0.14–0.16 | 41.32 | 0.18–0.22 | 25.83 | 0.25–0.43 | 10.33 |
| | 30~40 | 0.16–0.19 | 151.87 | 0.20–0.29 | 84.37 | 0.30–0.96 | 18.94 |
| | 40~50 | 0.40–0.49 | 41.61 | 0.50–0.89 | 41.6 | 1.00–3.23 | 0.89 |
| | 50~60 | 0.12–0.15 | 86.09 | 0.16–0.19 | 30.99 | 0.22–0.43 | 17.22 |
| B | 0~5 | 0.11–0.14 | 21.99 | 0.15–0.18 | 10.63 | 0.22–0.30 | 26.94 |
| | 5~10 | 0.12–0.15 | 38.22 | 0.16–0.19 | 21.74 | 0.22–0.43 | 63.03 |
| | 10~20 | 0.03–0.04 | 31.57 | 0.05–0.08 | 15.42 | 0.08–0.54 | 18.24 |
| | 20~30 | 0.34–0.39 | 33.29 | 0.43–0.56 | 17.83 | 0.68–0.96 | 10.74 |
| | 30~40 | 0.12–0.15 | 37.28 | 0.16–0.19 | 22.94 | 0.22–0.43 | 18.47 |
| | 40~50 | 0.32–0.39 | 25.83 | 0.40–0.59 | 14.35 | 0.63–1.67 | 3.21 |
| | 50~60 | 0.26–0.39 | 113.64 | 0.40–0.58 | 19.03 | 0.61–1.92 | 4.74 |
| C | 0~5 | 0.11–0.14 | 61.99 | 0.15–0.18 | 24.11 | 0.22–0.30 | 10.33 |
| | 5~10 | 0.43–0.59 | 21.93 | 0.61–0.96 | 15.83 | 1.05–2.36 | 12.73 |
| | 10~20 | 0.64–0.98 | 10.74 | 1.00–1.92 | 21.93 | 2.11–4.71 | 16.53 |
| | 20~30 | 0.03–0.04 | 33.72 | 0.05–0.09 | 11.63 | 0.11–0.54 | 19.83 |
| | 30~40 | 1.03–1.49 | 22.71 | 1.57–1.92 | 10.23 | 2.11–4.71 | 22.42 |
| | 40~50 | 0.14–0.19 | 60.26 | 0.22–0.30 | 19.8 | 0.35–0.61 | 5.17 |
| | 50~60 | 0.87–0.98 | 2.61 | 1.00–1.92 | 3.41 | 2.11–4.71 | 0.22 |
| D | 0~5 | 0.22–0.29 | 53.38 | 0.30–0.39 | 13.77 | 0.43–0.96 | 5.17 |
| | 5~10 | 0.18–0.20 | 25.83 | 0.22–0.30 | 25.83 | 0.35–0.61 | 5.17 |
| | 10~20 | 0.22–0.29 | 94.53 | 0.30–0.39 | 28.41 | 0.41–0.96 | 11.19 |
| | 20~30 | 0.27–0.33 | 37.02 | 0.34–0.48 | 18.6 | 0.51–1.36 | 4.82 |
| | 30~40 | 0.39–0.48 | 8.61 | 0.51–0.68 | 3.79 | 0.79–1.36 | 1.03 |
| | 40~50 | 0.32–0.39 | 18.08 | 0.41–0.48 | 6.54 | 0.51–0.96 | 3.27 |
| | 50~60 | 0.21–0.29 | 60.61 | 0.30–0.39 | 13.77 | 0.43–0.96 | 5.17 |
| E | 0~5 | 0.35–0.48 | 29.7 | 0.50–0.96 | 9.81 | 1.11–1.92 | 0.52 |
| | 5~10 | 0.43–0.59 | 19.8 | 0.61–0.96 | 6.03 | 1.05–2.36 | 0.86 |
| | 10~20 | 0.64–0.98 | 18.47 | 1.00–1.92 | 3.41 | 2.11–4.71 | 0.22 |
| | 20~30 | 0.03–0.04 | 41.19 | 0.05–0.09 | 21.21 | 0.11–0.54 | 29.4 |
| | 30~40 | 1.03–1.49 | 2.67 | 1.57–1.92 | 0.43 | 2.11–4.71 | 0.22 |
| | 40~50 | 0.34–0.39 | 7.23 | 0.43–0.56 | 4.13 | 0.68–0.96 | 1.03 |
| | 50~60 | 0.38–0.48 | 10.85 | 0.51–0.96 | 4.65 | 1.36–3.33 | 0.34 |
| F | 0~5 | 0.32–0.39 | 33.58 | 0.40–0.58 | 19.03 | 0.61–1.92 | 4.74 |
| | 5~10 | 0.80–0.98 | 2.91 | 1.03–1.78 | 1.61 | 2.11–4.71 | 0.22 |
| | 10~20 | 0.21–0.29 | 108.48 | 0.30–0.48 | 34.95 | 0.51–1.36 | 4.82 |
| | 20~30 | 0.20–0.27 | 13.03 | 0.30–0.35 | 6.03 | 0.43–0.61 | 2.58 |
| | 30~40 | 0.20–0.28 | 70.25 | 0.30–0.38 | 14.64 | 0.41–0.79 | 6.03 |
| | 40~50 | 0.33–0.49 | 58.66 | 0.50–0.79 | 12.45 | 0.83–1.93 | 2.09 |
| | 50~60 | 0.19–0.22 | 15.5 | 0.25–0.30 | 9.61 | 0.43–0.50 | 1.72 |

partial to the left of the soil layer, where lots of plant roots were distributed, whereas the other areas had little or no plant roots. In the additional mining staining soil profile, Brilliant Blue was seen in parts of the coal gangue; this indicated that the weathering velocity of coal gangue was fast, and the preferential flow might move along with the pathways of plant roots and the internal preferential flow path of coal gangue.

The vertical variation of soil preferential flow

The dye coverage ratio decreased as the soil layer depth increased in the different plots. The sequence of the dye coverage ratio at a depth of 0~60 cm in the six plots followed the order of *R. pseudoacacia* (26.48%) > *U. pumila* (20.12%) > farmland (15.06%) > shrub (13.97%) > weeds (10.07%). For every plot, the maximum dye coverage ratio occurred in the 0~5 cm soil layer, which followed the order of *R. pseudoacacia* (90.37%) > *U. pumila* (79.84%) > mixed forest (65.37%) > farmland (44.36%) > shrub (41.54%) > weeds (38.38%). The dye coverage ratio under the arbor was greater than that under shrub and weeds; that is, the distribution of preferential flow reached a maximum in the soil surface. Compared with weeds, the distribution of the preferential flow was more uniform under forestland. The dye coverage ratio of the soil surface was relatively high and sometimes reached 90%. The dye coverage ratio decreased with increasing soil depth, which decreased rapidly at a depth of 40 cm and closed to 0 at a depth of 60 cm.

The linear and inverse function regression equation was used to discuss the vertical variation of the preferential morphological flow characteristics. The relationship between the dye coverage ratio ($y$) and soil depth ($x$) was used to develop a regression analysis for the observation profile of the six plots (Table 4).

The fitting effects were good in different plots; the $R^2$ values were greater than 0.651, and the $P$ values were lower than 0.05, indicating that the fitting analysis results were consistent with the actual situation (Table 4). The fitting effect of the linear function was better than that of the inverse function. For the linear function, the $R^2$ ranged from 0.784 to 0.910, with an average of 0.86, and the $P$ values was less than 0.01; however, for the inverse function, the $R^2$ values ranged from 0.651 to 0.972, with an average value of 0.805, and the $P$ values were less than 0.05. Therefore, the linear function had a better fitting effect, which could be used to forecast and simulate the dyeing area, pathways, and frontal movement of the soil preferential flow in the dump, and has good practical guiding significance.

The influencing factors of soil preferential flow

A correlation matrix of the Pearson correlation coefficient was used to analyze the correlations between the environmental factors (soil, water, and plant factors) and the dye coverage ratio (Table 5). The soil factors include the soil bulk density, total porosity, capillary porosity, non-capillary porosity, average soil radius, gravel content, sand content, silt content, and clay content. The water factors include the soil water content and saturated hydraulic conductivity. The plant factors include the root weight density, <1 mm root length density, 1~2 mm root length density, and 2~5 mm root length density. A total of 15 environmental factors were taken into account (Table 5).

The dye coverage ratio of soil preferential flow under different vegetation reclamation types was very significantly positive correlated with the gravel content, the

**Table 4** The relationship between the dye coverage ratio ($y$) and the soil depth ($x$)

| Plots | $y = ax + b$ | | | | $y = a + b/x$ | | | |
|---|---|---|---|---|---|---|---|---|
| | Equations | $R^2$ | F | P | Equations | $R^2$ | F | P |
| A | $y = -1.600x + 82.914$ | 0.910 | 50.456 | 0.001 | $y = 5.511 + 444.521/x$ | 0.742 | 14.345 | 0.013 |
| B | $y = -1.653x + 85.266$ | 0.830 | 24.488 | 0.004 | $y = 2.007 + 511.029/x$ | 0.838 | 25.874 | 0.004 |
| C | $y = -1.173x + 63.930$ | 0.902 | 45.908 | 0.001 | $y = 6.178 + 341.878/x$ | 0.809 | 21.217 | 0.006 |
| D | $y = -0.648x + 33.250$ | 0.784 | 18.174 | 0.008 | $y = -0.747 + 221.856/x$ | 0.972 | 171.310 | 0.000 |
| E | $y = -0.893x + 47.880$ | 0.876 | 35.342 | 0.002 | $y = 5.377 + 236.976/x$ | 0.651 | 9.324 | 0.028 |
| F | $y = -0.608x + 33.335$ | 0.860 | 30.714 | 0.003 | $y = 3.053 + 182.692/x$ | 0.820 | 22.845 | 0.005 |

**Table 5** Spearman correlation between the dye coverage ratio and the environmental factors

| Environmental factors | | Correlation coefficient | Two-tailed significances | Sample number (N) |
|---|---|---|---|---|
| Soil factors | Sand content (%) | 0.157 | 0.351 | 126 |
| | Silt content (%) | −0.046 | 0.770 | 126 |
| | Clay content (%) | −0.163 | 0.303 | 126 |
| | Gravel content (%) | 0.767** | 0.000 | 126 |
| | Soil bulk density (g cm$^{-3}$) | −0.475** | 0.001 | 126 |
| | Total porosity (%) | 0.136 | 0.390 | 126 |
| | Capillary porosity (%) | −0.073 | 0.647 | 126 |
| | Non-capillary porosity (%) | 0.095 | 0.550 | 126 |
| | Mean radius of soil macropores (mm) | 0.619** | 0.000 | 126 |
| Water factors | Soil water content (%) | −0.415** | 0.006 | 126 |
| | Saturated hydraulic conductivity (mm min$^{-1}$) | 0.902** | 0.000 | 126 |
| Vegetation factors | Root weight density (g cm$^{-3}$) | 0.770** | 0.000 | 72 |
| | <1 mm root length density (cm cm$^{-3}$) | 0.599** | 0.002 | 72 |
| | 1~2 mm root length density (cm cm$^{-3}$) | 0.448* | 0.028 | 72 |
| | 2~5 mm root length density (cm cm$^{-3}$) | 0.414* | 0.044 | 72 |

*$P<0.05$, **$P<0.01$

mean radius of the soil macropores, the soil saturated hydraulic conductivity, the root weight density, and the <1 mm root length density ($P < 0.01$), which were very significantly negatively correlated with the soil bulk density and soil water content ($P < 0.01$). It was significantly positive correlated with the 1~2 mm root length density and 2~5 mm root length density ($P < 0.05$) but had no correlation with the remaining environment factors ($P > 0.05$).

*Soil factors*

(1)  Gravel content

The gravel content at the dump ranged from 45.34 to 89.81%, with an average of 69.02%, and the coefficient of variation was 15.86%, which belongs to weak variability (Fig. 7). The gravel content in different plots had a significant positive correlation with the dye coverage ratio. The dye coverage ratio increased with increasing gravel content. The gravel content in the circles, which was in the lower part of the line, was relatively high, whereas the dye coverage ratio was not very large. This indicated that much water passed along near the gravel and thus reduced the dye coverage ratio. If these data were removed, the gravel content would be reduced, and the gravel content and the dye coverage ratio would

have better correlation; thus, the effect of the gravel content on the soil preferential flow was verified.

(2)  Average radius of soil macropores

The average soil macropore radius for different reclaimed vegetation types at the dump ranged from 0.08 to 2.22 mm, the mean was 0.773 mm, and the coefficient of variation was 81.98%, which indicates medium variation (Fig. 7). The average radius of the soil macropores in different plots exhibited a significant positive correlation with the dye coverage ratio, and the staining area ratio increased with increasing average radius of the soil macropore. This indicated that some of the average soil macropore radius ranged from 1.5 to 2.5 mm and that both the average soil macropore radius and the corresponding staining area ratio were large. The greater the average soil macropore radius was, the bigger the staining area ratio where the soil preferential flow occurred.

(3)  Soil bulk density

The soil bulk density under different reclaimed vegetation types at the dump ranged from 1.12 to 1.49 g cm$^{-3}$, the mean value was 1.30 g cm$^{-3}$, and the coefficient of variation was 7.82%, which belongs to weak variation (Fig. 7). The soil bulk density under different plots exhibited a significant negative correlation with the dye coverage ratio.

The staining area ratio decreased with increasing soil bulk density.

*Water factors*

(1)   Soil saturated hydraulic conductivity

The saturated hydraulic conductivity ranged from 0.24 to 5.86 mm min$^{-1}$, the average value was 1.49 mm min$^{-1}$, and the coefficient of variation was 73.89%, which indicates medium variation (Fig. 8). The soil saturated hydraulic conductivity in different plots exhibited a significant positive correlation with the dye coverage ratio; the staining area ratio increased with increasing soil saturated hydraulic conductivity. The saturated hydraulic conductivity and the dye coverage ratio of the five data points, which formed a circle near the straight line, were greater. This indicated that the greater the saturated hydraulic conductivity was, the lager the dye coverage ratio where the soil preferential flow occurred.

(2)   Soil water content

The soil water content ranged from 4.9 to 19.55%, the average value was 13.20%, and the coefficient of variation was 23.08%, which represents medium variation (Fig. 8). The dye coverage ratio in different plots decreased with increasing soil water content.

*Plant factors*

(1)   Root weight density

The root weight density at the dump ranged from 0.0102 to 0.7076 g cm$^{-3}$, the mean value was 0.1576 g cm$^{-3}$, and the coefficient of variation was 118.20%, which represents strong variation (Fig. 9). This indicated that the vegetation root growth in each plot was affected by the soil structure and nutrient conditions. The root weight density in the different plots exhibited a significant positive correlation with the dye coverage ratio, and the dye coverage ratio increased with increasing root weight density.

(2)   Root length density

The root length density of different reclamation vegetations ranged from 0.0007 to 0.0354 cm cm$^{-3}$, the mean value was 0.00985 cm cm$^{-3}$, and the coefficient of variation was 88.22%, which represents medium variation (Fig. 9). The <1 mm root length density accounted for 68.97~100% of all the root length density. The root length density in the different plots had a significant positive correlation with the dye coverage ratio. Compared with the 1~2 mm and 2~5 mm root length densities, the dye coverage ratio had a higher correlation with the <1 mm root length density. The root length between 0.005 and 0.015 mm had a higher dye coverage ratio.

## Discussion

Soil macropores were one of the basic physical soil properties and the main reasons for the formation of preferential flow, which also affected the soil hydrological cycle, such as surface runoff, soil water infiltration, and groundwater distribution. However, there was no uniform standard of the definition of a soil macropore and the scope of soil pore size. Germann and Beven (1981), Vermeul et al. (1993), Bouma et al. (1977), Warner et al. (1989), and Singh et al. (1991) defined the size of the soil macropores as >0.03, >0.085, >0.1, >1, and >1.6 mm, respectively. Liu et al. (2001), Shi and Liu (2005), Feng and Hao (2002), and Li et al. (2007) also defined the size of soil macropores as >0.03 mm, 0.03~3 mm, >0.188 mm, and >1 mm, respectively. Typically, the size of the soil macropores ranged from 0.03 to 3 mm, most of which was concentrated in the 0.3~3 mm (Lv et al. 2012; Shi et al. 2005; Shi et al. 2008; Wang et al. 2010). This indicated that the dump was mixed with soil and rock, which belonged to the reconstructed soil. The soil pore structure of the dump changed greatly after the dumping process, such as mechanical leveling off, rolling, soil covering, and other methods, after which the function of soil and water conservation was influenced. Wang et al. (2016) found that the pore volume and porosity of reclaimed dump soil were reduced by large mechanical compaction, especially the volume and porosity of the soil macropores. The soil macropores under natural forest ranged from 0.4 to 2.3 mm (Shi et al. 2008), 0.3~3.0 mm (Wang et al. 2010), and 0.5~2.3 mm (Lv et al. 2012). In the present study, the radius of the soil macropores under different reclaimed vegetations

ranged from 0.03 to 4.71 mm; most radius ranged from 0.11 to 2.36 mm, which was lower than 0.3 to 3.0 mm. This indicated that the quantity and scope of the soil macropores decreased from compaction, which was consistent with Wang et al. (2016). Most previous studies have focused on forest soil under natural forestland, which has a better soil genetic horizon. However, the research object in the present study included the soil under reclaimed vegetation and the coal gangue layer (the upper layer was compacted reclaimed soil, and the lower layer was coal gangue with no soil structure). At the same time, the extreme climate, soil conditions, and soil water conditions led to the deaths of some reclaimed vegetation and many rotten roots. The mixture effects of coal gangue and plant roots affected the development of soil macropores and soil water movement.

The soil water movement was affected by the scope and radius of the soil macropores at the dump. In the present study, the minimum radius of the soil macropores in reclaimed soil occurred at a depth of 20~30 cm. The minimum radius value was 0.03 mm, which was consistent with the general recognition of the scope of the soil macropores. Thus, the minimum radius of the soil macropores was defined as 0.03 mm in the present study. The maximum radius of the soil macropores was distributed on the soil surface or in part of the deep soil, and the value was 4.71 mm, which was greater than that on forestland (3 mm) and farmland (2.8 mm). This was due to the soil macropores of forest soil resulting from the tree roots and the channels of animal activity, whereas the soil macropores on farmland were mostly caused by crop roots, surface tillage, and the application of manure. Öhrström et al. (2004) and Lipsius and Mooney (2006) noted that plant roots were one of the main factors affecting the formation of soil macropores. Stewart et al. (1999) found that soil macropores were concentrated in the vicinity of plant roots, the quantity of which could reach 80% of the total soil macropores. However, the scope of soil macropores in the coal gangue layer was too large, and this was not only caused by plant roots and animal channels but also related to the weathering degree of coal gangue. Related research found that the hydrological characteristics of coal gangue include poor structure, large porosity, poor soil water retention and fertilizer-retaining ability, and high permeability, in which it was easier to induce vertical erosion (Gao et al. 2006; Hu 1995; Zhang et al. 2008). The weathering degree of coal gangue was greater than that

of natural soil (Gao et al. 2006; Hu et al. 1993). Combined with soil profile pictures, the larger radius of soil macropores was mainly distributed at the site with serious weathering of coal gangue. The soil water moved along the priority pathway within the weathered coal gangue, which resulted in a corresponding larger scope and numbers of soil macropores. Related studies have found that soil macropores only occupied 5% of the total soil volume, whereas they still determined 67.4~77.0% of the variation in the steady effluent rate (Lv et al. 2012; Shi and Liu 2005; Shi et al. 2008) and 50~75% of the variance of the saturated hydraulic conductivity (Lv et al. 2012; Shi et al. 2005). In the present study, there was a very significant positive correlation between the average radius of the soil macropores with the steady effluent rate and saturated hydraulic conductivity ($P < 0.01$). The soil macroporosity for different reclaimed dump vegetations ranged from 0.03 to 16.58% and determined 65% of the variation in the steady effluent rate and 42% of the variation in the saturated hydraulic conductivity, both of which were lower than in the previous results. This was due to the dump soil having no soil genetic horizon and being mixed with gravel, coal gangue, and plant roots. Thus, the formation of soil macropores and the soil water movement were affected.

The reclaimed dump soil included loose deposits, which were caused by artificial accumulation through different reconstruction processes. A large amount of gravel and coal gangue could form macropores or tubular channels of a few centimeters, which resulted in the formation and distribution of soil preferential flow, which was different than that under forest soil. A large amount of water and nutrients moved rapidly along the preferential flow path to the deep soil, which resulted in a soil water deficit and nutrient loss and induced geological disasters such as collapse, landslides, and debris flows. This can hinder the recovery and improvement of land productivity. Warner et al. (1989) found that plant root systems and the sedimentary structure of coal gangue were the main factors influencing the movement of preferential flow in reclaimed mine forestland. In a previous study, there were significant differences in the characteristics of preferential flow between the soil layer and the weathering layer of coal gangue. In the soil layer, the dye coverage ratio (0~30 cm) ranged from 21.46 to 57.20%, while that in the weathering layer of coal gangue (30–60 cm) ranged from 3.84 to 9.12%. There were two reasons for this phenomenon. First,

compared with the gangue layer, the soil layer had better soil structure and more developed vegetation roots, which promoted the occurrence and development of preferential flow to a certain degree. Second, the structure of coal gangue became loose after the 8 years of weathering, and most of the soil water moved within the coal gangue, where Brilliant Blue existed inside, which could have been verified by the soil profile pictures. Rainfall, temperature, plant biomass, and human factors were the main factors affecting the weathering degree of coal gangue (Allaire-Leung et al. 2000), which then influenced the morphological characteristics of the preferential flow of reclaimed areas. Thus, the effects of the weathering degree of coal gangue on the characteristics, influencing factors, and mechanisms of preferential flow still require systematic study.

The factors influencing preferential flow in dumps were complex. Related research found that plant roots had an important influence on the formation and development of the soil macropores in forest soil (Allaire-Leung et al. 2000; Beven and Germann 1982; Lipsius and Mooney 2006). The soil structure changed as a result of the interpenetration and extension of roots. The size and connectivity of soil macropores were directly affected by the number, length, diameter, surface area, and volume of roots. Meanwhile, the effects of root holes (Gaiser 1952; Gish et al. 1998), animal activity channels (Green and Askew 1965; Murphy and Banfield 1978), human activities (tillage) (Li et al. 2002; Omoti and Wild 1979; Miao et al. 2011; Kong et al. 2015), and soil fissures caused by wet-dry cycles (Bouma 1981; Bouma and WÒSten 1984) and freezing-thawing cycles (Beven and Germann 1982; Ou et al. 1999) were the key factors affecting soil macropores, which further affected the path and distribution of preferential flow and then affected soil water and solute transport. De Vries and Chow (1978) found that the movement of preferential flow caused by soil macropores was faster and deeper than others, which was also the main reason for the formation of interflow. Furthermore, the gravel content (Green and Askew 1965; Li et al. 2002; Murphy and Banfield 1978) and rainfall intensity (Omoti and Wild 1979) were also the main factors affecting preferential flow. In the present study, a total of 15 environmental factors, including soil, water, and plant factors, were selected to evaluate the preferential flow of reclaimed soil. The dye coverage ratio of preferential flow for different reclamation vegetations was significant and positively correlated

with the root weight density, root length density, gravel content, average radius of the soil macropores, and soil saturated hydraulic conductivity, which promoted the formation and development of preferential flow. Among them, the effects of plant roots on preferential flow were more obvious than other factors. The dye coverage ratio of the preferential flow increased with increasing root weight density and root length density. The dye coverage ratio had a very significant positive correlation with the root weight density and had a significant positive correlation with the <1 mm root length density. Zhang et al. (2015) found that the fine roots (<1 mm) made a higher contribution to the preferential flow, which reached 94.8%. The gravel content also had a significant effect on the preferential flow. However, the increase in gravel content was bad for soil and water conservation and promoted soil water and nutrient loss. Thus, appropriate measures should be taken to reduce the impact of gravel content on preferential flow. In the future, the quantitative effects of various environmental factors on preferential flow should be strengthened, and an evaluation index system of preferential flow in reclamation areas should be determined, which could provide a scientific basis for the study of preferential flow systems, soil hydrological processes and hydrological effects, and regional vegetation restoration and reconstruction at the dump.

## Conclusions

There were differences in the soil water breakthrough curve on different plots, which could be divided into three stages: an active period, a fluctuation period, and a stable period. The soil macropore effluent rate generally increased first and then tended toward a stable state. The steady effluent rates under *R. pseudoacacia*, *U. pumila*, and mixed forests (*R. pseudoacacia* and *U. pumila*) at a depth of 0~5 cm were 0.0281, 0.0292, and 0.0315 mm s$^{-1}$, respectively, while the rates under shrub, farmland, and weeds were lower than 0.02 mm s$^{-1}$. The soil steady effluent rate decreased with increasing soil depth and reached the maximum and minimum values at the depths of 0~5 cm (0.0193~0.0315 mm s$^{-1}$) and 50~60 cm (0.0028~0.0035 mm s$^{-1}$), respectively. Furthermore, the radius of soil macropores under different reclaimed vegetations ranged from 0.03 to 4.71 mm, most of which ranged from 0.11 to 2.36 mm. There were no

significant differences in the radius and the number of soil macropores in the different soil layers under all of the six plots. The scope of the soil macropore radius in the lower soil was greater than that in the upper layer. The soil macroporosity for different reclaimed vegetations ranged from 0.03 to 16.58%, which determined 65% of the variation in the steady effluent rate and 42% of the variation in the saturated hydraulic conductivity. Furthermore, the dye coverage ratio under different plots followed the order of *R. pseudoacacia* (26.48%) > *U. pumila* (20.12%) > mixed forests (17.32%) > farmland (15.06%) > shrub (13.97%) > weeds (10.07%). The preferential flow at each plot mostly occurred at a depth of 0~40 cm, which occupied 98.54% (A), 98.12% (B), 93.93% (C), 98.53% (D), 97.09% (E), and 98.71% (F) of the whole soil profile (0~60 cm). The dye coverage ratio decreased rapidly at a depth of 40 cm and reached 0 at a depth of 60 cm. The dye coverage ratio under arbors was greater than that under shrubs and weeds. There was a better linear relationship between the dye coverage ratio and soil depth ($y = ax + b$), and the determination coefficient $R^2$ was greater than 0.78. Moreover, the Pearson correlation was used to analyze the relationship between the environmental factors (soil, water, and plant factors) and the dye coverage ratio. The dye coverage ratio of the soil preferential flow for different reclaimed vegetations was very significantly or significantly positively correlated with the gravel content, mean radius of the soil macropores, soil saturated hydraulic conductivity, root weight density, and root length density ($P < 0.01$), which was also significantly positive correlated with the 1~2 mm and 2~5 mm root length densities ($P < 0.05$). This promoted the formation and development of soil preferential flow. The dye coverage ratio was very significantly negatively correlated with the soil bulk density and soil water content ($P < 0.01$).

# References

Allaire-Leung, S. E., Gupta, S. C., & Moncrief, J. F. (2000). Water and solute movement in soil as influenced by macropore characteristics: 1. Macropore continuity. *Journal of Contaminant Hydrology, 41*(3), 283–301.

Bauters, T. W. J., Steenhuis, T. S., DiCarlo, D. A., Nieberc, J. L., Dekkerd, L. W., Ritsemad, C. J., Parlangea, J. Y., & Haverkampe, R. (2000). Physics of water repellent soils. *Journal of Hydrology, 231*, 233–243.

Beven, K., & Germann, P. (1982). Macropores and water flow in soils. *Water Resources Research, 18*(5), 1311–1325.

Bouma, J. (1981). Soil morphology and preferential flow along macropores. *Agricultural Water Management, 3*(4), 235–250.

Bouma, J., Jongerius, A., Boersma, O., Jager, O., & Schoonderbeek, D. (1977). The function of different types of macropores during saturated flow through four swelling soil horizons. *Soil Science Society of America Journal, 41*(5), 945–950.

Bouma, J., & WÒSten, J. H. M. (1984). Characterizing ponded infiltration in a dry cracked clay soil. *Journal of Hydrology, 69*(1–4), 297–304.

Cheng, Y., Zhang, H. J., Shi, Y. H., Wang, Y. J., Sheng, Q. L., Chang, D. D., Kitahara, H., & Wang, Z. Z. (2001). Spatial variability of pipes in granite slope in the Three Gorges of Yangtze River. *Journal of Beijing Forestry University, 23*(5), 19–22 (in Chinese).

Clothier, B. E., Green, S. R., & Deurer, M. (2008). Preferential flow and transport in soil: progress and prognosis. *European Journal of Soil Science, 59*(1), 2–13.

De Vries, J., & Chow, T. L. (1978). Hydrologic behavior of a forested mountain soil in coastal British Columbia. *Water Resources Research, 14*(5), 935–942.

Dušek, J., Vogel, T., Lichner, L., Čipáková, A., & Dohnal, M. (2006). Simulated cadmium transport in macroporous soil during heavy rainstorm using dual-permeability approach. *Biologia, 61*(19), S251–S254.

Feng, J., & Hao, Z. C. (2002). Distribution of soil macropores characterized by CT. *Advances in Water Science, 13*(5), 611–617 (in Chinese).

Flury, M., Flühler, H., Jury, W. A., & Leuenberger, J. (1994). Susceptibility of soils to preferential flow of water: a field study. *Water Resources Research, 30*(7), 1945–1954.

Forrer, I., Papritz, A., Kasteel, R., Flühler, H., & Luca, D. (2000). Quantifying dye tracers in soil profiles by image processing. *European Journal of Soil Science, 51*(2), 313–322.

Gaiser, R. N. (1952). Root channels and roots in forest soils. *Soil Science Society of America Journal, 16*(1), 62–65.

Gao, L. S., Xu, L., Yin, Z. D., Fan, J. S., & Zhou, X. C. (2006). Study on soil permeability of waste rock hill. *Research of Soil and Water Conservation, 13*(3), 45–46 (in Chinese).

Gazis, C., & Feng, X. (2004). A stable isotope study of soil water: evidence for mixing and preferential flow paths. *Geoderma, 119*(1), 97–111.

Germán-Heins, J., & Flury, M. (2000). Sorption of brilliant blue FCF in soils affected by pH and ionic strength. *Geoderma, 97*(1), 87–101.

Germann, P., & Beven, K. (1981). Water flow in soil macropores I. An experimental approach. *Journal of Soil Science, 32*, 1–13.

Gish, T. J., Gimenez, D., & Rawls, W. J. (1998). Impact of roots on ground water quality. *Plant and Soil, 200*(1), 47–54.

Glass, R. J., Steenhuis, T. S., & Parlange, J. Y. (1988). Wetting front instability as a rapid and far-reaching hydrologic

process in the vadose zone. *Journal of Contaminant Hydrology, 3*(2), 207–226.

Green, R. D., & Askew, G. P. (1965). Observations on the biological development of macropores in soils of Romney Marsh. *Journal of Soil Science, 16*(2), 342–344.

Hagedorn, F., & Bundt, M. (2002). The age of preferential flow paths. *Geoderma, 108*(1), 119–132.

Hangen, E., Gerke, H. H., Schaaf, W., & Hüttl, R. F. (2005). Assessment of preferential flow processes in a forest-reclaimed lignitic mine soil by multicell sampling of drainage water and three tracers. *Journal of Hydrology, 303*(1), 16–37.

Hendrickx, J. M., & Flury, M. (2001). Uniform and preferential flow mechanisms in the vadose zone. *Conceptual models of flow and transport in the fractured vadose zone*, 149–187.

Herrick, J. E., Van Zee, J. W., Belnap, J., Johansen, J. R., & Remmenga, M. (2010). Fine gravel controls hydrologic and erodibility responses to trampling disturbance for coarse-textured soils with weak cyanobacterial crusts. *Catena, 83*(2), 119–126.

Hu, Z. Q. (1995). Afforestation of waste pile in semi-arid areas. *Journal of China Coal Society, 20*(3), 322–327 (in Chinese).

Hu, Z. Q., Li, Y., Li, J. M., & Mao, Y. (1993). Moisture characteristic of coal waste pile and its afforestation. *Energy Environmental Protection, 4*, 25–28 (in Chinese).

Institute of Soil Science, Chinese Academy of Sciences. (1978). Soil physical and chemical analysis (p. 66–70). Beijing: Science Press (in Chinese).

Jomaa, S., Barry, D. A., Brovelli, A., Heng, B. C. P., Sander, G. C., Parlange, J. Y., & Rose, C. W. (2012). Rain splash soil erosion estimation in the presence of rock fragments. *Catena, 92*, 38–48.

Jørgensen, P. R., Hoffmann, M., Kistrup, J. P., Bryde, C., Bossi, R., & Villholth, K. G. (2002). Preferential flow and pesticide transport in a clay-rich till: field, laboratory, and modeling analysis. *Water Resources Research, 38*(11), 1–15.

Koestel, J. K., Moeys, J., & Jarvis, N. J. (2012). Meta-analysis of the effects of soil properties, site factors and experimental conditions on solute transport. *Hydrology and Earth System Sciences, 16*(6), 1647–1665.

Kong, D. X., Miao, C. Y., Borthwick, A. G. L., Duan, Q. Y., Liu, H., Sun, Q. H., Ye, A. Z., Di, Z. H., & Gong, W. (2015b). Evolution of the Yellow River Delta and its relationship with runoff and sediment load from 1983 to 2011. *Journal of Hydrology, 520*, 157–167.

Larsson, M. H., Jarvis, N. J., Torstensson, G., & Kasteel, R. (1999). Quantifying the impact of preferential flow on solute transport to tile drains in a sandy field soil. *Journal of Hydrology, 215*(1), 116–134.

Li, W. L., Jin, C. J., Wang, A. Z., Pei, T. F., & Guan, D. X. (2007). Characteristics of macropores in two forest soils on northern slope of Changbai Mountains. *Chinese Journal of Applied Ecology, 18*(6), 1213–1218 (in Chinese).

Li, D. C., Velde, B., Delerue, J. F., & Zhang, T. L. (2002). Digital image analysis on the evolution of soil structure under no tillage system. *Acta Pedologica Sinica, 39*(2), 214–220 (in Chinese).

Lipsius, K., & Mooney, S. J. (2006). Using image analysis of tracer staining to examine the infiltration patterns in a water repellent contaminated sandy soil. *Geoderma, 136*(3), 865–875.

Liu, W., Ou, Z. Q., & Ying, P. F. (2001). Soil macropore and its studying methodology. *Chinese Journal of Applied Ecology, 12*(3), 465–468 (in Chinese).

Luxmoore, R. J. (1981). Micro-, meso-, and macroporosity of soil. *Soil Science Society of America Journal, 45*(3), 671–672.

Luxmoore, R. J., Jardine, P. M., Wilson, G. V., Jones, J. R., & Zelazny, L. W. (1990). Physical and chemical controls of preferred path flow through a forested hillslope. *Geoderma, 46*(1), 139–154.

Lv, G., Wang, H. L., & Huang, L. (2012). A study on macropore properties of forest soil in semi-arid region of western Liaoning province. *Bulletin of Soil and Water Conservation, 32*(5), 176–181 (in Chinese).

Miao, C. Y., Ashouri, H., Hsu, K., Sorooshian, S., & Duan, Q. Y. (2015). Evaluation of the PERSIANN-CDR daily rainfall estimates in capturing the behavior of extreme precipitation events over China. *Journal of Hydrometeorology, 16*, 1387–1396.

Miao, C. Y., Borthwick, N. J. R., Alistair, G. L., & Yang, L. (2011). A preliminary estimate of human and natural contributions to the changes in water discharge and sediment load in the Yellow River. *Global and Planetary Change, 76*(3–4), 196–205.

Miao, C. Y., Kong, D. X., Wu, J. W., & Duan, Q. Y. (2016b). Functional degradation of the water–sediment regulation scheme in the lower Yellow River: spatial and temporal analyses. *Science of the Total Environment, 551-552*, 16–22.

Miao, C. Y., Su, L., Sun, Q. H., & Duan, Q. Y. (2016a). A nonstationary bias-correction technique to remove bias in GCM simulations. *Journal of Geophysical Research, 121*(10), 5718–5735.

Murphy, C. P., & Banfield, C. F. (1978). Pore space variability in a sub-surface horizon of two soils. *Journal of Soil Science, 29*(2), 156–166.

Öhrström, P., Hamed, Y., Persson, M., & Berndtsson, R. (2004). Characterizing unsaturated solute transport by simultaneous use of dye and bromide. *Journal of Hydrology, 289*(1), 23–35.

Omoti, U., & Wild, A. (1979). Use of fluorescent dyes to mark the pathways of solute movement through soils under leaching conditions: 2. Field experiments. *Soil Science, 128*(2), 98–104.

Ou, Z., Jia, L., Jin, H., Yediler, A., Jiang, X., Kettrup, A., & Sun, T. (1999). Formation of soil macropores and preferential migration of linear alkylbenzene sulfonate (LAS) in soils. *Chemosphere, 38*(9), 1985–1996.

Radulovich, R. (1989). Soil macropore size distribution from water breakthrough curves. *Soil Science Society of America Journal, 53*(2), 556–559.

Shi, H., Chen, F. Q., & Liu, S. R. (2005). Macropores properties of forest soil and its influence on water effluent in the upper reaches of Minjiang River. *Acta Ecologica Sinica, 25*(3), 507–512 (in Chinese).

Shi, H., & Liu, S. R. (2005). The macroporosity properties of forest soil and its eco-hydrological significance. *Journal of Mountain Research, 23*(5), 533–539 (in Chinese).

Shi, Z. J., Wang, Y. H., Xu, L. H., Xiong, W., Yu, P. T., Guo, H., & Xu, D. P. (2008). The influence of rock fragments on the characteristics of macropore and water effluent of forest soils in the Liupan Mountains, Northwest China. *Acta Ecologica Sinica, 28*(10), 4929–4939 (in Chinese).

Singh, P., Kanwar, R. S., & Thompson, M. L. (1991). Measurement and characterization of macropores by using AUTOCAD and automatic image analysis. *Journal of Environmental Quality, 20*(1), 289–294.

Stewart, J. B., Moran, C. J., & Wood, J. T. (1999). Macropore sheath: quantification of plant root and soil macropore association. *Plant and Soil, 211*(1), 59–67.

Vermeul, V. R., Istok, J. D., Flint, A. L., & Pikul, J. L. (1993). An improved method for quantifying soil macroporosity. *Soil Science Society of America Journal, 57*(3), 809–816.

Wang, J. M., Guo, L. L., Bai, Z. K., Qin, Q., & Lv, C. J. (2016). Effects of land reclamation time on soil pore number and porosity based on computed tomography (CT) images in opencast coal mine dump. *Transactions of the Chinese Society of Agricultural Engineering, 32*(12), 229–236 (in Chinese).

Wang, Q., Yang, W., & Liu, W. (1999). Adsorption of acetanilide herbicides on soils and its correlation with soil properties. *Pesticide Science, 55*(11), 1103–1108.

Wang, K., & Zhang, R. (2011). Heterogeneous soil water flow and macropores described with combined tracers of dye and iodine. *Journal of Hydrology, 397*(1–2), 105–117.

Wang, W., Zhang, H. J., Cheng, J. H., Wu, Y. H., Du, S. C., & Wang, R. (2010). Macropore characteristics and its relationships with the preferential flow in broadleaved forest soils of Simian Mountains. *Chinese Journal of Applied Ecology, 21*(5), 1217–1223 (in Chinese).

Warner, G. S., Nieber, J. L., Moore, I. D., & Geise, R. A. (1989). Characterizing macropores in soil by computed tomography. *Soil Science Society of America Journal, 53*(3), 653–660.

Yan, J., & Zhao, W. (2016). Characteristics of preferential flow during simulated rainfall events in an arid region of China. *Environmental Earth Sciences, 75*(7), 1–12.

Zavala, L. M., González, F. A., & Jordán, A. (2009). Fire-induced soil water repellency under different vegetation types along the Atlantic dune coast-line in SW Spain. *Catena, 79*(2), 153–162.

Zhang, H., Cheng, J., Shi, Y., & Cheng, Y. (2007). The distribution of preferential paths and its relation to the soil characteristics in The Three Gorges Area, China. *International Journal of Sediment Research, 22*(1), 39–48.

Zhang, Z. B., Lin, L., Wang, Y., & Peng, X. H. (2016b). Temporal change in soil macropores measured using tension infiltrometer under different land uses and slope positions in subtropical China. *Journal of Soils and Sediments, 16*(3), 854–863.

Zhang, Y. H., Niu, J. Z., Zhu, W. L., Han, Y. N., Du, X. Q., & Chen, S. J. (2015). Effects of plant root systems on preferential flow in forest ecosystems. *Acta Ecologica Sinica, 35*(6), 1788–1797 (in Chinese).

Zhang, R., Zhang, C. L., Li, M. S., Zhang, H. J., & Cheng, J. H. (2008). Research on water dynamics of weathered coal gangue dumps. *Bulletin of Soil and Water Conservation, 28*(1), 124–129 (in Chinese).

Zhang, Y. H., Zhang, M. X., Niu, J. Z., & Zheng, H. J. (2016a). The preferential flow of soil: A widespread phenomenon in pedological perspectives. *Eurasian Soil Science, 49*(6), 661–672.